# Aluminum partitioning during phase separation in Fe-20%Cr-6%Al ODS alloy

C. Capdevila*, M.K. Miller**, K.F. Russell**

* Centro Nacional de Investigaciones Metalúrgicas (CENIM), Consejo Superior de Investigaciones científicas (CSIC), Avda. Gregorio del Amo, 8; Madrid, E-28040, Spain
** Materials Science and Technology Division, Oak Ridge National Laboratory, Oak Ridge, TN 37831-6136, USA

Keywords: phase separation, solute partitioning, PM 2000 oxide dispersion strengthened steel

## Abstract

Phase separation in a commercial Fe-20 wt% Cr-6% Al oxide dispersion-strengthened PM 2000 steel has been characterized with a local-electrode atom probe after isothermal ageing at 708 and 748 K for times up to 3600 h. A progressing decrease in the Al content of the Cr-rich $\alpha'$ phase was observed with time at both ageing temperatures. The Al partitioning trend was consistent with theoretical calculations. However, the experimentally observed Al partitioning factor was significantly lower than the predicted equilibrium value. A ~10 nm diameter, roughly spherical, Al- and Ti-enriched $\beta'$ Fe(AlTi) phase was also observed.

## Introduction

PM 2000™ is a Fe – 20 wt% Cr – 6% Al oxide dispersion strengthened (ODS) ferritic steel that is manufactured at Plansee GmbH by a complex powder metallurgy route for high-temperature applications. Typical applications of PM 2000 include shields or carrier systems in furnace construction, stirrers and plungers in molten glass in the glass industry, thermocouple protection tubes, burner tubes, and a variety of parts used in high-temperature testing-equipment, the combustion of waste materials, and automotive diesel engines. PM 2000 is now also being used in the manufacture of rotating discs for glass fiber production, high temperature screws and fasteners, fact sheets in thermal-protection panels, and space and aerospace engineering in general [1, 2]. Moreover, PM 2000 sheet has been used in combustion chambers for turbines and for burner hardware in coal and oil burning power stations. Although this alloy has wide-ranging applications, the main uses of PM 2000 are in applications where a combination of creep strength and oxidation resistance at high temperatures is of paramount importance [3]. Thus, PM 2000 contains chromium and aluminum for corrosion and oxidation resistance, and yttrium for creep strength.

Experiments performed with pre-oxidized PM 2000 revealed an increase in hardness when the alloy was annealed at 748 K (475 ºC). This hardness increase is consistent with the so-called "475 ºC embrittlement" that is characteristic of high-chromium ferritic steels. This phenomenon has been attributed to phase separation within a low temperature miscibility gap to form Fe-rich $\alpha$ and Cr-rich $\alpha'$ phases [4-6].

Limited experimental data are available on the role of Al during phase separation within the low temperature miscibility gap in PM 2000. Read and Murakami reported that insignificant Al partitioning occurred after ageing for 598 h at 748K in a Fe-20 wt% Cr-4.5% Al-0.5% Ti + 0.5% $Y_2O_3$ alloy, MA956 [7]. However in a later study of the same

MA956 alloy, Read et al. detected Al partitioning to the α phase after extending the ageing time to 2900 h and stated that the observed Al partitioning behavior only occurred when there was a sufficient driving force at the later stages of phase separation of Cr in Fe [12]. Aluminum partitioning was observed during phase separation of Fe-30% Cr-14% Co-2% Al after ageing for 2 h at 798 K [8], although the decomposition behavior of the system will be modified by higher Cr content and Co addition. This study investigates the distribution of Al that occurs during low-temperature ageing of PM 2000 with particular focus on the α and α′ phases.

**Materials and experimental techniques**

The chemical composition of the PM 2000 alloy used in this study, as determined by X-ray Fluorescence (XRF), is given in Table 1. The PM 2000 alloy used was provided by Plansee GmbH in the form of as-rolled bars. PM 2000 is a Fe – 20% Cr – 6% Al, yttria dispersion-strengthened steel manufactured by a mechanical alloying process. In this process, elemental powders or compounds are heavily deformed together in a ball mill to such large strains that the powder particles become solid solutions. The alloyed powder is then canned, hot-extruded, and hot rolled into bar.

The microstructure of the as-extruded and hot rolled condition consists of fine (~0.5 μm) equiaxed grains. The alloy was subsequently annealed at a temperature of ~0.9 of the melting-point of the alloy (1633 K for 3 h) and cooled in a switched-off furnace. This heat treatment ensures that all the Cr and Ti and almost all of the Al are in solid solution in the ferritic matrix. After this treatment, the grains coarsen into strongly elongated columnar grains parallel to the extrusion direction (several millimeters in length with a grain aspect ratio of 5). The microstructure also contains a distribution of aluminum-yttrium oxides preferentially aligned along the extrusion direction. This

microstructure is suitable for high-temperature applications. Subsequent low temperature isothermal ageing treatments were conducted at 708 and 748 K for times between 10 and 3600 h.

Needle-shaped specimens for atom-probe tomography were cut from bulk material and electropolished with the use of the standard double layer and micropolishing methods [9]. In some cases, focused ion-beam (FIB) milling was used in the final stages of sample preparation. This FIB technique was found to result in longer specimen lifetimes during analysis. Atom probe analyses were performed in the ORNL local electrode atom probe (LEAP®) manufactured by Imago Scientific Instruments. The local electrode atom probe was operated with a specimen temperature of 60K, a pulse repetition rate of 200 kHz, and a pulse fraction of 0.2.

## Results and discussion

### *Thermodynamic calculations*

The position of the miscibility gap in a Fe-Cr system is shown in Figure 1. Free energy changes of the system ($\Delta G_M$) curves were calculated from the Scientific Group Thermodata Europe (SGTE) solution databases and only considered the existence of body centered cubic (bcc) phases. The miscibility gap corresponds to the minima of $\Delta G_M$ versus Cr-content curve. Superimposed on the theoretical calculations are the experimental Mössbauer and resistivity data obtained by Kuwano [10, 11] for several Fe-Cr alloys.

The low-temperature miscibility gap in the binary Fe-Cr bcc phase field extends to the ternary Fe-Cr-Al system. Therefore, the theoretical calculations performed on the binary Fe-Cr system were extended to the ternary Fe-Cr-Al system with 11 at. % Al and a Fe-Cr-Al-Ti with 11 at.% Al and 0.5 at.% Ti (Figure 1). It is clear that the addition of 0.5

at. % Ti has almost no influence on the miscibility gap. The yttria addition was ignored in calculations although the formation of mixed Y-Al-Ti oxides will deplete the matrix of some solute additions. Moreover, the loss of some Al, Ti and Fe to form a Fe(AlTi) intermetallic compound, described below, was also ignored. These calculations indicated that the critical temperature of the miscibility gap, $T_{Cr}$, is lowered from 898 K to 885 K with the addition of 11 at. % Al. The predicted compositions of equilibrium α and α′ phases at 708 and 748 K in the Fe – Cr – Al system are given in Table 2. From partitioning coefficients shown in Table 2, Al was predicted to partition strongly to the α phase, and the partitioning factor increases with decreasing temperature. The addition of up to 11 at.% Al also suppresses the competing but extremely sluggish-forming σ phase [12].

***Phase separation and solute partitioning***

Phase separation within the low-temperature miscibility gap occurred in the PM 2000 alloy during both isothermal ageing treatments to form Fe-rich α and Cr-rich α′ phases. Atom probe tomography revealed that aluminum partitioning occurred between the α and α′ phases after ageing for 3600 h at 708 K, as shown in the atom maps in Figure 2 and a composition profile in Figure 3. Similar results were obtained after ageing for 3600 h at 748 K, as shown in the atom maps in Figure 4 and a composition profile in Figure 5. The location of these atom maps and composition profile were selected to also show an ~10 nm diameter, roughly spherical Al- and Ti- enriched phase. The Al- and Ti- enriched phase was present in a significantly lower number density compared to the α′ phase. The number density of β′ precipitates at both temperatures tested was estimated to be $1 \times 10^{22}$ $m^{-3}$. The Al- and Ti-enriched phase corresponds to the B2-ordered β′ FeAl phase with the Ti substituting for the Al (as it does in $Ni_3Al$). This β′

phase is also the basis of the iron-based superalloys (Fe-Al-Ni-Mo) that was shown to have an approximate composition of 51% Al, 38% Ni and 11% Fe [13]. An interesting observation is the common interface between the α′ and β´ phases. The co-development and morphology of the α′ and β´ phases will be described in detail elsewhere.

The evolution of compositions of the α and α′ phases during ageing at 708 and 748 K were evaluated with the use of proximity histograms [14]. The change in the Al content across the α-α′ interface in PM 2000 after ageing at 708 and 748 K is shown in Figure 6. The phase compositions and the $c^{\alpha}_{Al}/c^{\alpha'}_{Al}$ partitioning factors are listed in Tables 3 and 4 for the 708 and 748 K treatments, respectively. For all ageing times, the measured Al concentrations in the α phase were similar to those theoretically predicted values. The results from both ageing temperatures reveal a progressive decrease in Al content in the α′ phase resulting in an increase in the $c^{\alpha}_{Al}/c^{\alpha'}_{Al}$ partitioning factor with time. However, even for the longest ageing times, neither the Cr nor the Al levels in the α′ phase attained the predicted values. Consequently, the partitioning factors of 3.8 and 4.3 are significantly smaller than the predicted equilibrium values of 21.1 and 14.7 at 708 and 748 K, respectively. This result suggests that the phases have not attained their equilibrium levels after ageing for 3600 h. Although the results exhibit scatter due to the low levels of both elements, the $c^{\alpha'}_{Fe}/c^{\alpha'}_{Al}$ ratios were similar at each ageing temperature. The change in the $c^{\alpha}_{Al}/c^{\alpha'}_{Al}$ partitioning factor with the chromium content of the α′ phase is shown in Figure 7. These results indicate that as the chromium content of the α′ phase increases with ageing time, the aluminum and iron are rejected from the α′ phase. The Al rejected from the α′ phase will be consumed in the Fe(Al,Ti) β′ phase.

## Conclusions

This atom probe tomography study has clearly detected a progressive depletion of Al from the Cr-rich α′ phase in a PM 2000 alloy during isothermal ageing at 708 and 748 K for times between 10 and 3600 h. This experimental result is consistent with the expected trend from theoretical predictions. Although the Al depletion occurs more rapidly at 748 K than at 708 K, the calculated $c_{Al}^{\alpha} / c_{Al}^{\alpha'}$ partitioning ratio is far higher than the one measured, even after 3600 h, which suggests that equilibrium levels have not been attained. An Al- and Ti-enriched phase corresponding to the B2-ordered β′ (Fe(Al,Ti)) phase has been detected during ageing at 708 and 748 K.

## Acknowledgements

The authors acknowledge financial support from the Spanish Ministerio de Educación y Ciencia in the form of a Coordinate Project in the Energy Area of Plan Nacional 2006 (ENE2006-15170-C02). Research at the Oak Ridge National Laboratory SHaRE User Facility was sponsored by Basic Energy Sciences, U.S. Department of Energy. PM 2000™ is a trademark of Plansee SE.

## References

[1] P. SCHADE and L. BARTHA, Int. J. Refract. Met. Hard Mater. 24 (2006) 273.
[2] R. SCHAUBLIN, A. RAMAR, N. BALUC, V. DE CASTRO, M. A. MONGE, T. LEGUEY, N. SCHMID and C. BONJOUR, J. Nucl. Mater. 351 (2006) 247.
[3] C. CAPDEVILA, U. MILLER, H. JELENAK and H. BHADESHIA, Mater. Sci. Eng. A 316 (2001) 161.
[4] M. J. BLACKBURN and J. NUTTING, J. Iron Steel Inst. 202 (1964) 610.
[5] R. LAGNEBORG, ASM Transactions Quarterly 60 (1967) 67.
[6] A. PLUMTREE and R. GULLBERG, Metall. Trans. A 7A (1976) 1451.
[7] H. G. READ, H. MURAKAMI and K. HONO, Scripta Mater. 36 (1997) 355.

[8] F. ZHU, H. WENDT and P. HAASEN, Scr. Metall. 16 (1982) 1175.
[9] M. K. MILLER, in "Atom Probe Tomography", (Kluwer Academic / Plenum Press, New York, 2000) p. 28.
[10] H. KUWANO, Trans. Jpn. Inst. Met. 26 (1985) 721.
[11] H. KUWANO, Trans. Jpn. Inst. Met. 26 (1985) 730.
[12] S. M. DUBIEL and G. INDEN, Z. MetaIlkd. 78 (1987) 544.
[13] M. K. MILLER, M. G. HETHERINGTON, J. R. WEERTMAN and H. A. CALDERON, in "Alloy Phase Stability and Design", edited by G. M. Stocks, D. P. Pope and A. F. Giamei (MRS, Pittsburgh, PA 1991) p. 219.
[14] O. C. HELLMAN, J. A. VANDENBROUCKE, J. RÜSING, D. ISHEIM and D. N. SEIDMAN, Microsc. Microanal. 6 (2000) 437.

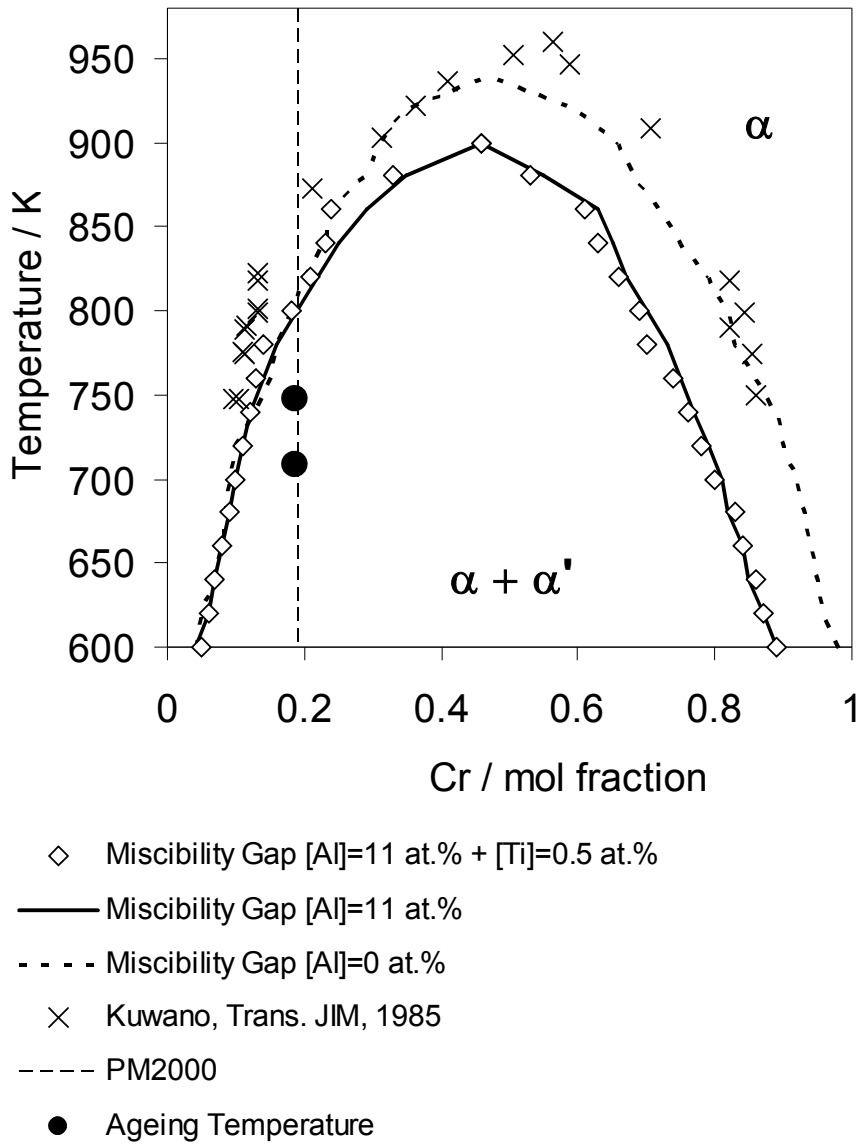


Figure 1. Influence of additions of 11 at. % Al and 0.5 at. % Ti to Fe-Cr system on the miscibility gap ($\alpha$ is the Fe-rich and $\alpha'$ is the Cr-rich bcc phases). Vertical dashed line corresponds to the PM 2000 alloy composition.

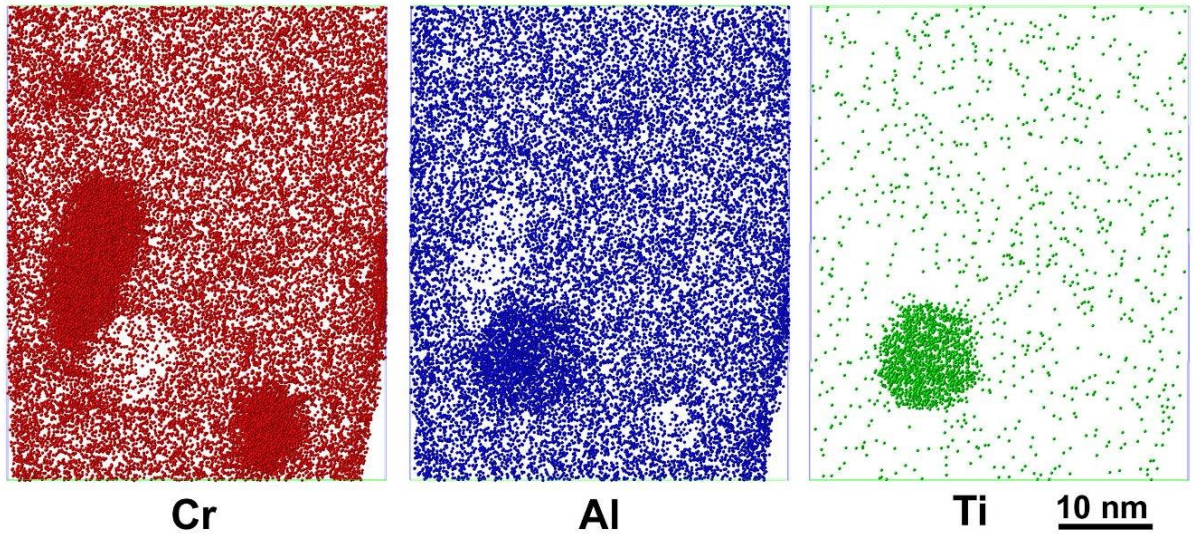


Figure 2. Atom maps of the microstructure of PM 2000 aged at 708 K for 3600 h showing the Al depletion in the Cr-enriched α′ phase (higher density/darker regions in the Cr atom map). An ~10-nm diameter Al- and Ti-enriched β′ precipitate is also evident. The selected volume represented is 40 × 40 in extent by 4 nm thick

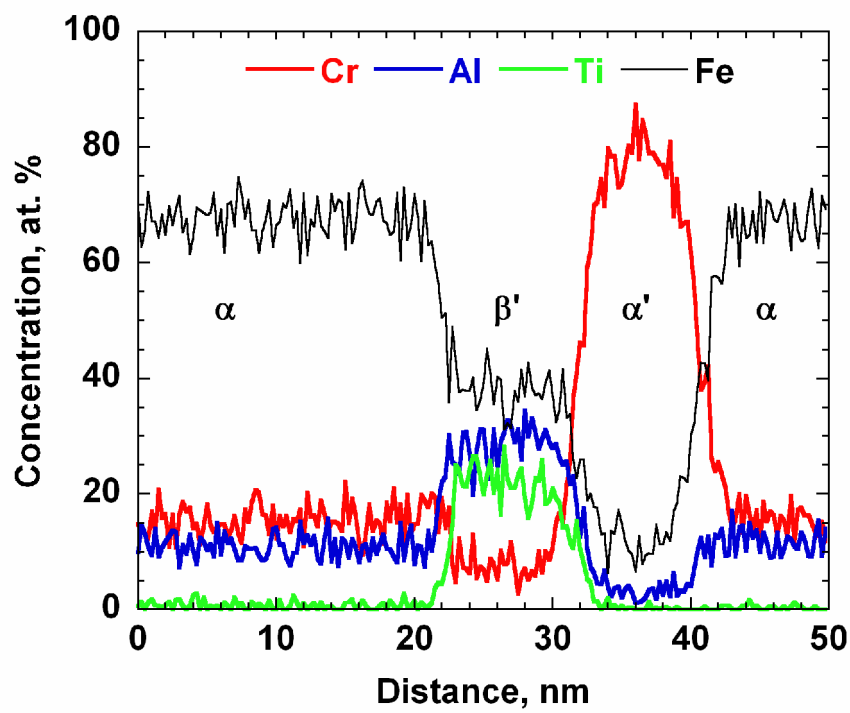


Figure 3. Concentration profiles across the α′ phase and an Fe(Al,Ti) β′ particle in PM 2000 aged at 708 K for 3600 h showing the Al depletion in the Cr-enriched α′ phase.

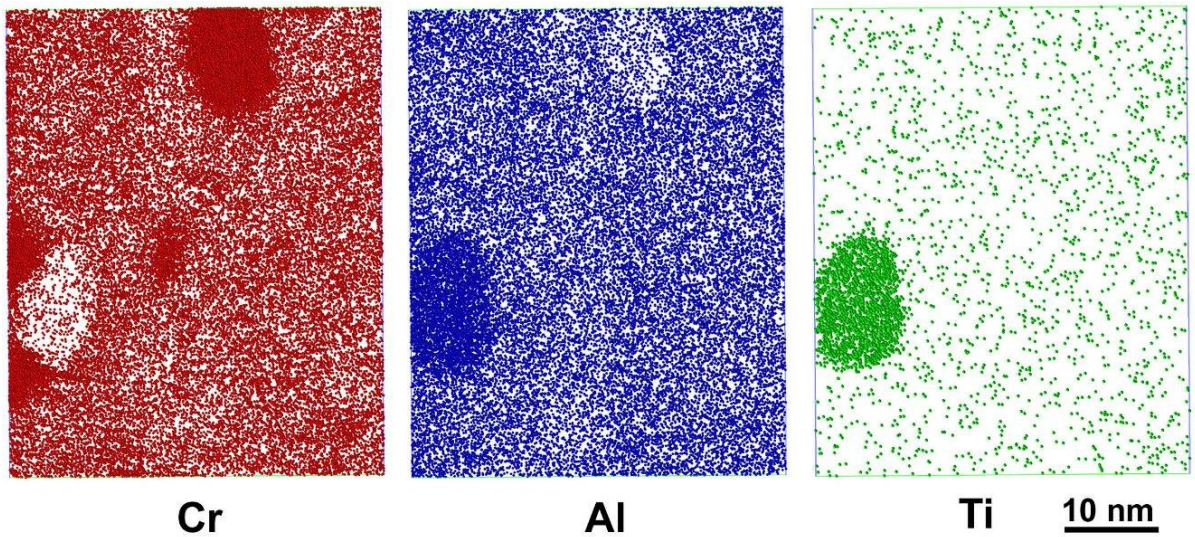


Figure 4. Atom maps of the microstructure of PM 2000 aged at 748 K for 3600 h showing the Al depletion in the Cr-enriched α′ phase (higher density/darker regions in the Cr atom map). An ~10-nm diameter Al- and Ti-enriched β′ precipitate is also evident. The selected volume represented is 40 × 40 in extent by 4 nm thick

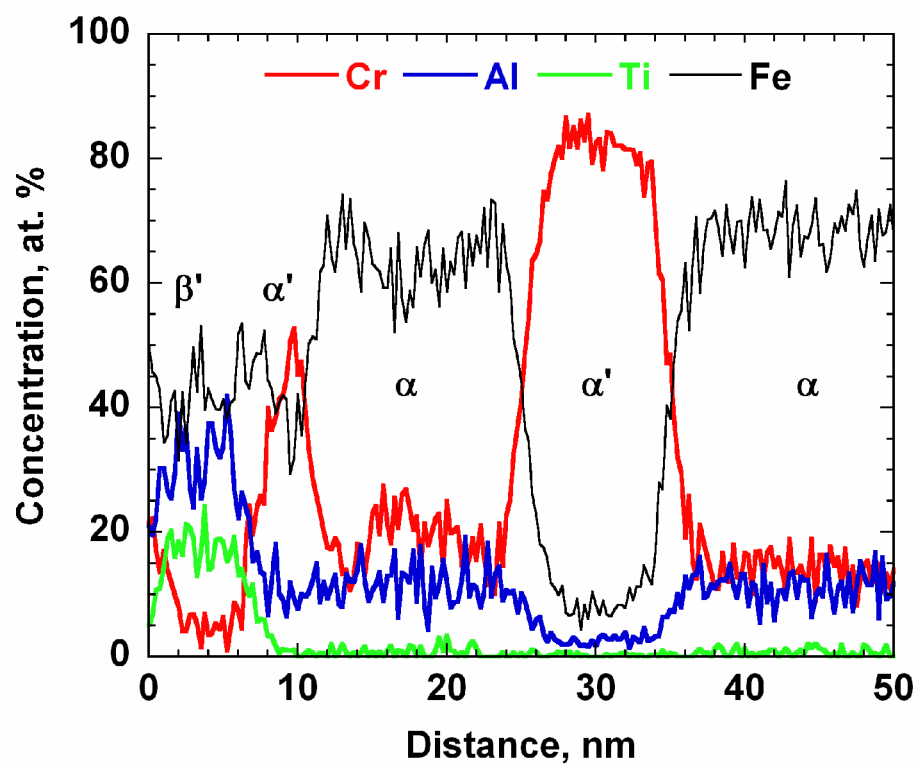


Figure 5. Concentration profiles across α′-phase and an Fe(Al,Ti) particle after ageing at 748 K for 3600 h showing the Al depletion in the Cr-enriched α′ phase.

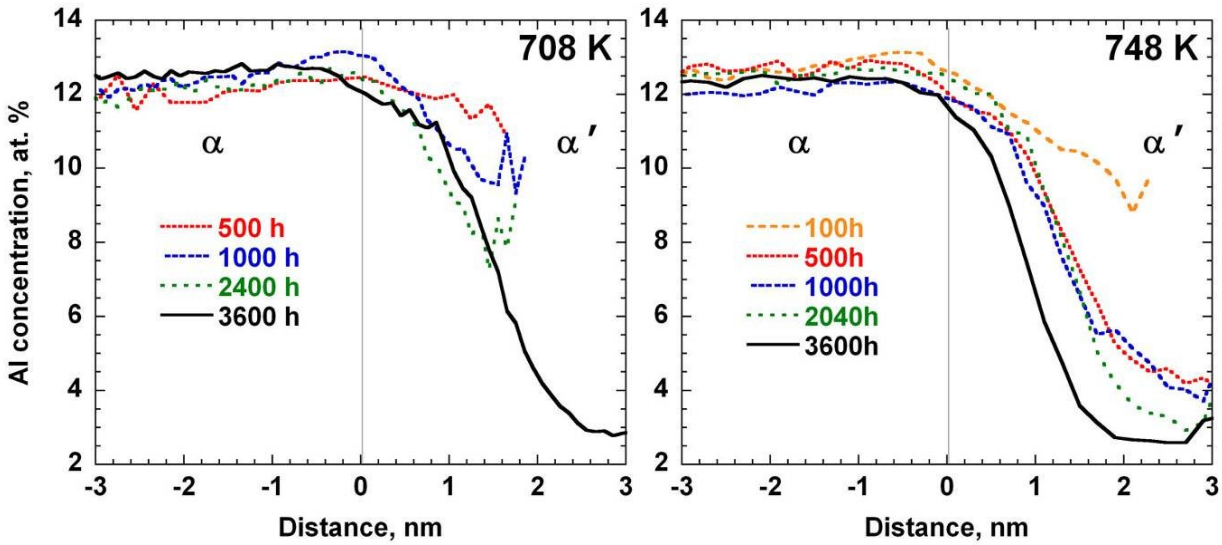


Figure 6. Al proximity histograms across the α-α′ interface in PM 2000 after ageing at 708 and 748 K showing the progressive reduction of Al content in the α′ phase with time.

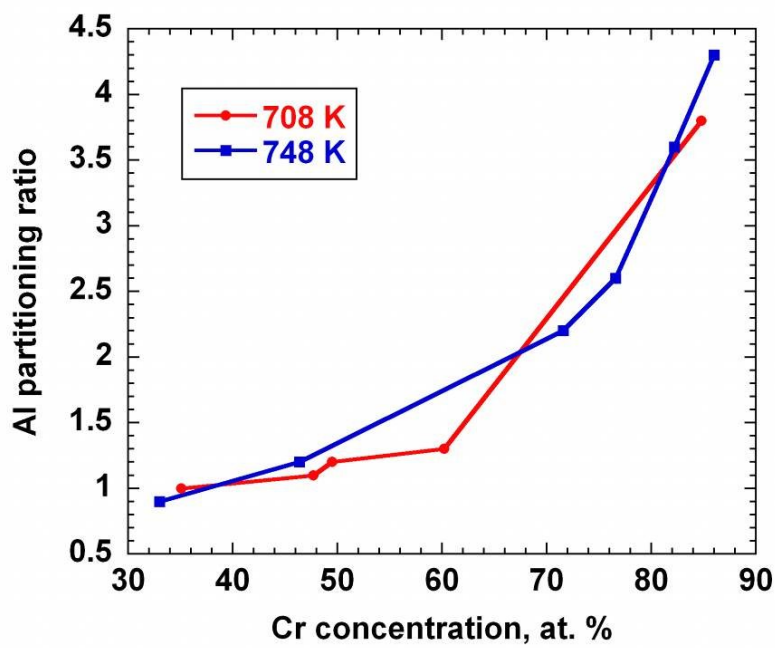


Figure 7. Al partitioning ratio between the α and α′ phases as a function of the Cr content of the α′ phase in PM 2000 after ageing at 708 and 748 K.

Table 1. Chemical composition as determined by XRF of the PM 2000 alloy used in this study. The balance is iron.

| | Cr | Al | Ti | C | O | N | Y |
|---|---|---|---|---|---|---|---|
| wt. % | 18.6 | 5.2 | 0.54 | 0.04 | 0.09 | 0.006 | 0.39 |
| at. % | 18.5 | 10.1 | 0.58 | 0.17 | 0.28 | 0.022 | 0.23 |

Table 2 Calculated equilibrium phase composition in Fe – Cr – Al system equivalent to PM 2000

| Solute | Fe-rich α (at. %) | Cr-rich α′ (at. %) |
|---|---|---|
| | T = 748 K | |
| Fe | 78.2 | 7.0 |
| Cr | 8.6 | 92.1 |
| Al | 13.2 | 0.9 |
| $c^{\alpha}_{Al} / c^{\alpha'}_{Al}$ | 14.7 | |
| | T = 708 K | |
| Fe | 80.1 | 4.96 |
| Cr | 6.43 | 94.4 |
| Al | 13.5 | 0.64 |
| $c^{\alpha}_{Al} / c^{\alpha'}_{Al}$ | 21.1 | |

Table 3. Compositions of the α and α′ phases for the different ageing times at 708 K as estimated from the proximity histogram. The balance of the analyses is iron.

| at. % | 100 h | 500 h | 1000 h | 2040 h | 3600 h |
|---|---|---|---|---|---|
| $Cr_{\alpha}$ | 16.7 | 18.3 | 19.2 | 17.7 | 15.6 |
| $Al_{\alpha}$ | 12.3 | 11.8 | 12.2 | 11.8 | 12.4 |
| $Ti_{\alpha}$ | 0.73 | 0.57 | 0.50 | 0.51 | 0.80 |
| $Cr_{\alpha'}$ | 35.1 | 47.7 | 49.5 | 60.2 | 84.8 |
| $Al_{\alpha'}$ | 11.8 | 10.8 | 10.6 | 8.90 | 3.21 |
| $Ti_{\alpha'}$ | 0.90 | 1.20 | 1.04 | 0.84 | 0.31 |
| $\Delta C_{Cr}$ | 18.4 | 29.4 | 30.3 | 42.4 | 69.1 |
| $c^{\alpha}_{Al} / c^{\alpha'}_{Al}$ | 1.0 | 1.1 | 1.2 | 1.3 | 3.8 |
| $c^{\alpha'}_{Fe} / c^{\alpha'}_{Al}$ | 4.4 | 3.7 | 3.7 | 3.4 | 3.6 |

Table 4. Compositions of the α and α′ phases for the different ageing times at 748 K as estimated from the proximity histogram. The balance of the analyses is iron.

| at. % | 10 h | 100 h | 500 h | 1000 h | 2040 h | 3600 h |
|---|---|---|---|---|---|---|
| $Cr_{\alpha}$ | 17.1 | 16.6 | 15.7 | 16.0 | 15.6 | 17.0 |
| $Al_{\alpha}$ | 12.2 | 12.6 | 12.6 | 11.9 | 12.5 | 12.3 |
| $Ti_{\alpha}$ | 0.62 | 0.63 | 0.75 | 0.44 | 0.48 | 0.70 |
| $Cr_{\alpha'}$ | 33.0 | 46.4 | 71.6 | 76.6 | 82.2 | 86.0 |
| $Al_{\alpha'}$ | 13.7 | 10.0 | 5.78 | 4.62 | 3.45 | 2.86 |
| $Ti_{\alpha'}$ | 0.44 | 0.39 | 0.27 | 0.16 | 0.12 | 0.32 |
| $\Delta C_{Cr}$ | 15.9 | 29.8 | 55.9 | 60.7 | 66.6 | 69.0 |
| $c^{\alpha}_{Al} / c^{\alpha'}_{Al}$ | 0.9 | 1.2 | 2.2 | 2.6 | 3.6 | 4.3 |
| $c^{\alpha'}_{Fe} / c^{\alpha'}_{Al}$ | 3.9 | 4.3 | 3.9 | 4.0 | 4.1 | 3.8 |